Journal of Medicinal Chemistry

ARTICLE

pubs.acs.org/jmc

Unsymmetrical Cyclotriazadisulfonamide (CADA) Compounds as Human CD4 Receptor Down-Modulating Agents

Violeta G. Demillo,[†] Florian Goulinet-Mateo,[†] Jessica Kim,[†] Dominique Schols,[‡] Kurt Vermeire,[‡] and Thomas W. Bell*[,†]

[†]Department of Chemistry, University of Nevada, Reno, Nevada 89557-0216, United States

[‡]Rega Institute for Medical Research, Katholieke Universiteit Leuven, B-3000 Leuven, Belgium

Supporting Information

ABSTRACT: Cyclotriazadisulfonamide (CADA) inhibits HIV at submicromolar levels by specifically down-modulating cell-surface and intracellular CD4. The specific biomolecular target of CADA compounds is unknown, but previous studies led to an unsymmetrical binding model. To test this model, methods were developed for effective synthesis of diverse, unsymmetrical CADA compounds. A total of 13 new, unsymmetrical target compounds were synthesized, as well as one symmetrical analogue. The new compounds display a wide range of potency for CD4 down-modulation in CHO·CD4-YFP cells. VGD020 (IC_{50} = 46 nM) is the most potent CADA compound discovered to date, and VGD029 (IC_{50} = 730 nM) is the most potent fluorescent analogue. Structure−activity relationships are analyzed from the standpoint of additive or nonadditive energy effects of different substituents. They appear to be consistent with the zipper-type mechanism in which entropy costs are reduced for additional stabilizing interactions between the small molecule and its protein target.

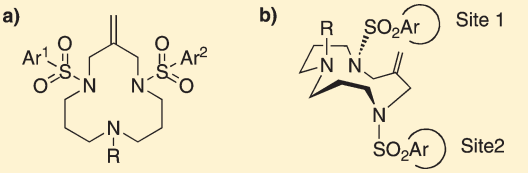

INTRODUCTION

The cluster of differentiation 4 (CD4) glycoprotein is mainly expressed on the surface of thymocytes, T-helper lymphocytes, and macrophage/monocyte cells.[1] This intercellular adhesion molecule plays a central role in the immune response via its function in several steps of physiological T-cell activation.[2,3] Accordingly, $CD4^+$ T cells are believed to be important in the pathogenesis of a variety of immunologically based diseases (e.g., asthma, rheumatoid arthritis, and diabetes), and anti-CD4 monoclonal antibodies have been explored as a therapeutic strategy for these diseases.[4−7] Anti-CD4 antibodies are also being explored for treatment of cutaneous T-cell lymphomas, since malignant cells express CD4 in all stages of disease progression.[8] CD4 is also the main receptor enabling infection by the human immunodeficiency virus (HIV), so it has become an important target for therapeutic intervention.[9−12] Viral entry inhibitors are actively being pursued as novel anti-HIV agents,[13−16] including anti-CD4 antibodies[17,18] and chemokine receptor antagonists.[19,20] Several studies have shown that down-modulation of CD4 effectively protects cells from HIV infection,[21−25] and this has even been found to be a strategy by which the African green monkey avoids progression to acquired immune deficiency syndrome (AIDS) after infection by simian immunodeficiency virus (SIV).[26]

The small molecule cyclotriazadisulfonamide (CADA, Figure 1) potently inhibits in vitro replication of a broad spectrum of HIV-1 strains, as well as HIV-2 and SIV, by down-modulating cell surface CD4.[27] Consistent with this entry-inhibitor mechanism of action, the anti-HIV effect of CADA is synergistic with those of antiviral drugs operating by other mechanisms, including inhibitors of HIV reverse transcriptase, protease, and attachment/entry.[28] Moreover, in a series of more than 25 CADA analogues, anti-HIV potency was directly correlated with CD4 down-modulation ability.[25] It was recently discovered that CADA inhibits the synthesis of functional CD4 by blocking cotranslational translocation of nascent CD4 across the endoplasmic reticulum (ER) membrane.[29] This effect is

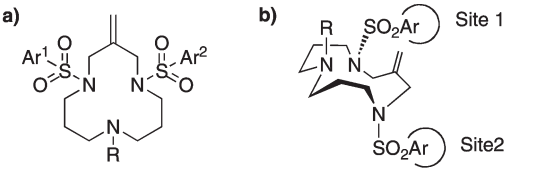

Compound	Ar^1	Ar^2	R	Potency
CADA	*p*-tolyl	*p*-tolyl	Bn	1
1 (QJ028)	*p*-tolyl	*p*-tolyl	$CH_2C_6H_{11}$	2.4
2 (KKD023)	4-MeOPh	4-MeOPh	Bn	3.6
3 (KKD015)	*p*-tolyl	dan*	Bn	0.6
4 (KKD016)	*p*-tolyl	dan*	$CH_2C_6H_{11}$	1.3

* dan = 1-(5-NMe_2naphthyl)

Figure 1. (a) Structures of previously synthesized CADA compounds, including unsymmetrical analogues **3** and **4**. (b) Proposed unsymmetrical two-site binding model. Potency = IC_{50}(CADA)/IC_{50}(compound). IC_{50} is for CD4 down-modulation in MT-4 cells (ref 30).

Received: March 6, 2011
Published: July 29, 2011

dx.doi.org/10.1021/jm2002603 | *J. Med. Chem.* 2011, 54, 5712–5721

Scheme 1

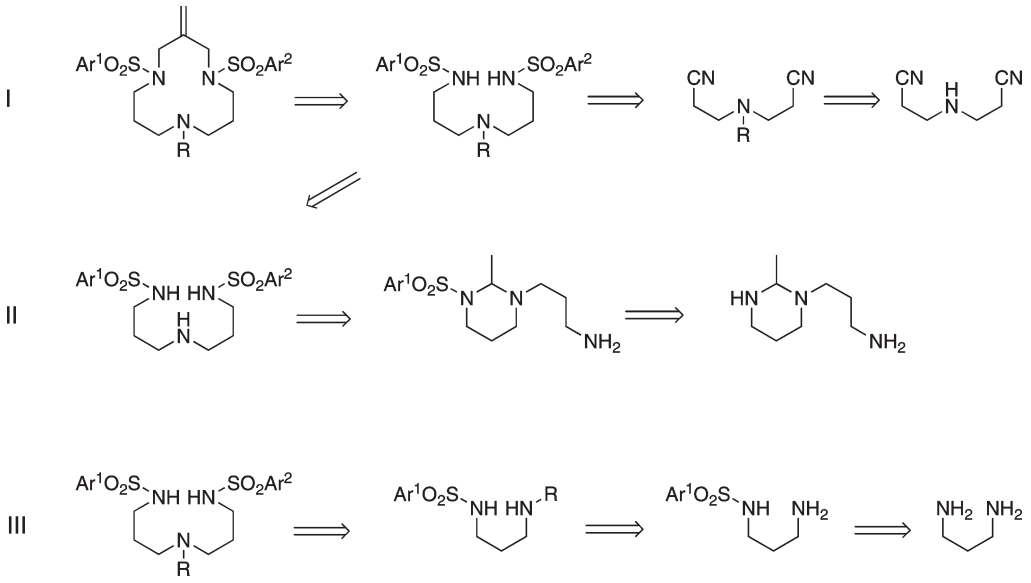

apparently specific for the CD4 signal peptide sequence, and it results in degradation of nascent CD4 in the cytosol.

Given that the specific biomolecular target of CADA compounds has not been identified, numerous analogues with different arenesulfonyl side arms and tail groups ($ArSO_2$ and R, respectively, as defined in Figure 1) have been synthesized and used to develop a 3D QSAR model for CD4 down-modulation.[30] Some interesting effects of these substitutions appear in the table in Figure 1. The column labeled "Potency" compares activities of the analogues with that of CADA ($IC_{50} \approx 0.8\ \mu M$). Two symmetrical analogues, **1** (QJ028)[25] and **2** (KKD023),[30] show that either substitution of the benzyl tail by cyclohexylmethyl or substitution of the *p*-tolyl groups of the side arms produces significant increases in potency. Replacement of one *p*-toluenesulfonyl side arm of either CADA or **1** with 5-dimethylaminonaphthalene-1-sulfonyl (dansyl) gave fluorescent probes[31] **3** (KKD015)[30] or **4** (KKD016),[30] respectively. The potencies of these unsymmetrical analogues are comparable to that of CADA, while the symmetrical didansyl analogue corresponding to **3** had no detectable activity (structure and data not shown).

The finding that one *p*-toluenesulfonyl (tosyl) side arm of CADA can be changed to a bulky dansyl group without strongly affecting potency, while the same replacement of both tosyl side arms destroys potency, led to the unsymmetrical binding-conformation model shown in Figure 1. This model is based on the unsymmetrical conformation observed in the X-ray crystal structures of CADA and three analogues, which was also used for aligning analogue structures for 3D QSAR analysis.[30] In these structures, the 12-membered ring is twisted about the isobutylene headgroup such that one sulfonamide nitrogen is approximately in the isobutylene plane and the other is out of this plane. This places the two arenesulfonyl side arms in very different orientations with respect to the macro ring. If this is the bioactive conformation of the drug, then the two side arms occupy quite different sites of the biomolecular target, labeled "Site 1" and "Site 2" in Figure 1. It stands to reason that these two sites may have very different size constraints and that only one can accommodate the bulky dansyl side arm. At the time of their synthesis, **3** and **4** were the only unsymmetrical CADA analogues known. The goal of the studies described here was mainly to explore other unsymmetrical compounds in order to test our "two-site" binding model and, hopefully, to discover more potent compounds.

RESULTS AND DISCUSSION

Synthesis. Three retrosynthetic pathways for symmetrical and unsymmetrical CADA compounds are shown in Scheme 1. All three use the same disconnection of the macrocyclic ring of the target molecule to an open-chain disulfonamide intermediate. This final step of the synthesis can be accomplished by Atkins–Richman macrocyclization[32,33] of the corresponding bis(tosylamide) dianion with 2-chloromethyl-3-chloropropene, as described previously for preparation of CADA compounds for structural and QSAR studies.[30] The Atkins–Richman macrocyclization requires large volumes of anhydrous DMF and gives limited yields because of the formation of byproducts and consequential losses in chromatographic purification. The syntheses reported here generally employ an improved, recently developed, palladium-catalyzed cyclization method.[34]

Previously reported symmetrical CADA compounds were prepared by pathway I in Scheme 1, as exemplified by the synthesis of **2** shown in Scheme 2[30] The requisite open-chain disulfonamide intermediate (**8**) was prepared from triamine **7**, which was obtained by reduction of bis(2-cyanoethyl)benzylamine (**6**), in turn prepared by benzylation of bis(cyanoethyl)amine (**5**). For purpose of comparison with the new, unsymmetrical compounds reported here, **2** was debenzylated with α-chloroethyl chloroformate (ACE-Cl)[35,36] and the resulting secondary amine, **9** (KKD025),[30] underwent reductive alkylation to give the novel symmetrical analogue **10** (VGD045).[37]

Synthesis of unsymmetrical CADA compounds requires access to unsymmetrical disulfonamide intermediates. Pathway II (Scheme 1) shows the route used for the preparation of unsymmetrical, dansyl-containing analogues **3** and **4**.[30] An inexpensive starting material, bis(3-aminopropyl)amine, was desymmetrized by condensation with acetaldehyde to form a cyclic aminal (a hexahydropyrimidine) bearing primary, secondary, and

dx.doi.org/10.1021/jm2002603 |*J. Med. Chem.* 2011, 54, 5712–5721

Scheme 2

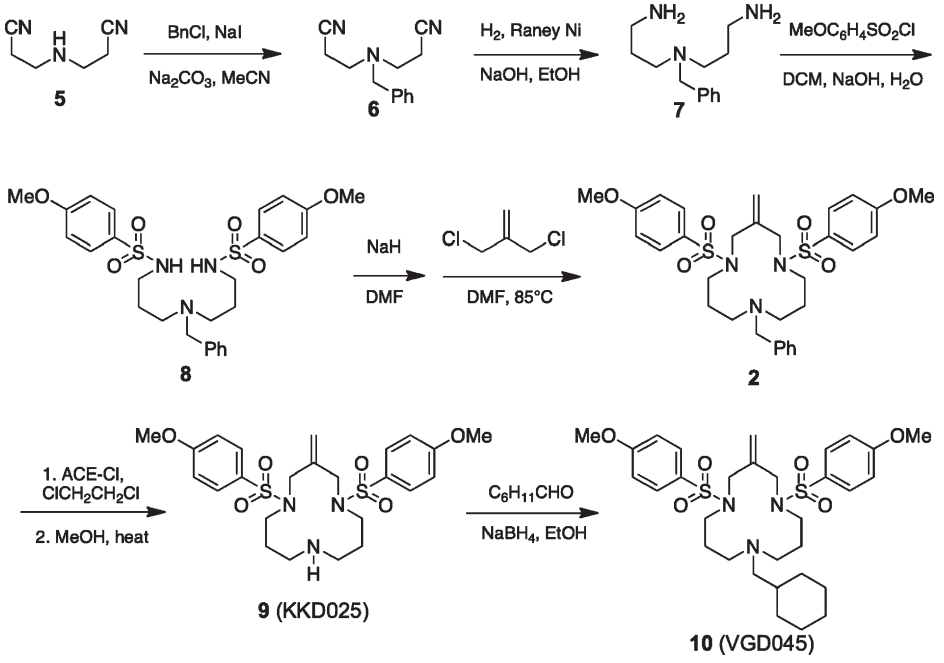

tertiary nitrogen atoms. Tosylation at the more nucleophilic secondary nitrogen followed by dansylation of the primary nitrogen and ring-opening proceeded in low yield (18% overall), but after installation of benzyl or cyclohexylmethyl tail groups and Atkins−Richman macrocyclization, the corresponding CADA analogues **3** and **4** were obtained.

A new approach to unsymmetrical CADA compounds is shown as retrosynthetic pathway III (Scheme 1). Here, the unsymmetrical disulfonamide intermediate is obtained by chain elongation of an *N*-alkyl-*N*-sulfonyl-1,3-diaminopropane. This intermediate, in turn, is prepared by reductive alkylation of a monotosyl or monodansyl derivative of 1,3-diaminopropane. Pathway III shares with pathway II the desymmetrization of an inexpensive starting material, but the new approach is more effective because yields are higher overall.

The syntheses of 12 new, unsymmetrical CADA compounds by pathway III are shown in Scheme 3.[37] For compounds in which one of the arenesulfonyl groups is tosyl (Ar^1 = *p*-tolyl), the synthesis began with reaction of tosyl chloride with an excess of 1,3-diaminopropane,[38,39] giving the monotosyl derivative (**11**) in 48% yield. While this is only a modest yield, the reactants are inexpensive and a low yield is best tolerated early in a synthesis. Dansylation of 1,3-diaminopropane gave monodansyl derivative **12** in 99% yield. Reductive alkylation of **11** and **12** by reaction with cyclohexanecarboxaldehyde and sodium borohydride gave the corresponding *N*-cyclohexylmethyl derivatives (**13** and **14**) in high yield. In the tosyl case (**13**), the crude product contained a minor impurity of the dialkylation side product, but this could be removed by chromatography at a later stage of the synthesis.

Eight new, unsymmetrical CADA compounds (**28**−**34** and **37**) were synthesized by the longer, five-step route shown in Scheme 3.[37] All of these bear a tosyl side arm (Ar^1 = *p*-tolyl) and were synthesized from diamine intermediate **13** by alkylation with 3-bromopropylphthalimide[40] to give intermediate **15** in 84% yield. Cleavage of the phthalimide protecting group with hydrazine gave triamine **16** (96%), which was sulfonylated with various arenesulfonyl chlorides to afford open-chain intermediates **17**−**23** and **26** in 34−78% yield, after purification by column chromatography. In some cases, the shorter, three-step route shown in Scheme 3 was compared. In one case, reaction of intermediate **13** with *N*-(3-bromopropyl)benzenesulfonamide (Ar^2 = phenyl) gave the corresponding open-chain triamine (**24**) in higher yield than was obtained overall for three steps via intermediates **15** and **16**. The two dansylated analogues **36** and **38** were also prepared via the shorter route by reaction of intermediate **14** with *N*-(3-bromopropyl)-4-methoxybenzenesulfonamide or *N*-(3-bromopropyl)-4-nitrobenzenesulfonamide to give open-chain intermediate **25** or **27**, respectively.

All of the 11 new unsymmetrical CADA compounds were prepared from the open-chain intermediates by a recently developed cyclization method using catalytic amounts of palladium(0) and 1,4-bis(diphenylphosphino)butane (dppb).[34] This reaction uses smaller amounts of a more volatile solvent (acetonitrile) and generally produces fewer byproducts than the Atkins−Richman method. Nevertheless, the yields of the pure macrocycles ranged widely (19−53%), apparently because of losses from repeated chromatographic separations required for complete purification in a few cases. A one-armed analogue, **39** (VGD040),[37] was also prepared by cleavage of the 2-nitrobenzenesulfonyl side arm of **26** with 2-mercaptoethanol.[41]

After the high potency of compound **31** (VGD020) was discovered, benzyl tail analogue **42** (VGD027)[37] was synthesized by the route shown in Scheme 4.[37] This parallels the shorter, three-step route to cyclohexylmethyl tail compounds shown in Scheme 3. Thus, the monotosyl derivative of 1,3-diaminopropane (**11**) was reductively alkylated with benzaldehyde to give **40** in 70% yield. Reaction of this diamine with *N*-(3-brompropyl)-4-methoxybenenesulfonamide gave open-chain triamine **41** (VGD026)[37] in 54% yield, after purification by column chromatography. Palladium catalyzed macrocyclization, followed by purification as the hydrochloride salt afforded pure **42**·HCl·H_2O in 56% yield.

dx.doi.org/10.1021/jm2002603 |*J. Med. Chem.* 2011, 54, 5712–5721

Scheme 3

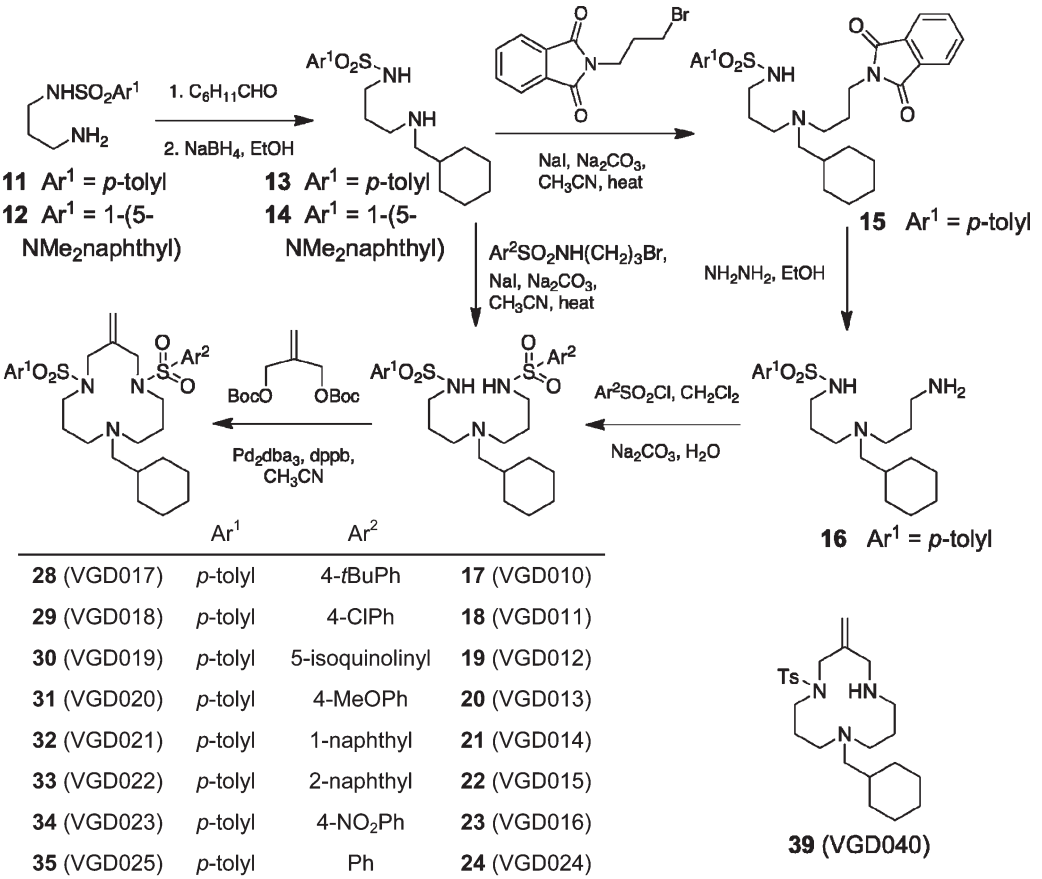

	Ar^1	Ar^2	
28 (VGD017)	*p*-tolyl	4-*t*BuPh	**17** (VGD010)
29 (VGD018)	*p*-tolyl	4-ClPh	**18** (VGD011)
30 (VGD019)	*p*-tolyl	5-isoquinolinyl	**19** (VGD012)
31 (VGD020)	*p*-tolyl	4-MeOPh	**20** (VGD013)
32 (VGD021)	*p*-tolyl	1-naphthyl	**21** (VGD014)
33 (VGD022)	*p*-tolyl	2-naphthyl	**22** (VGD015)
34 (VGD023)	*p*-tolyl	4-NO_2Ph	**23** (VGD016)
35 (VGD025)	*p*-tolyl	Ph	**24** (VGD024)
36 (VGD029)	dan*	4-MeOPh	**25** (VGD028)
37 (VGD039)	*p*-tolyl	2-NO_2Ph	**26** (VGD038)
38 (VGD049)	dan*	4-NO_2Ph	**27** (VGD048)

*dan = 1-(5-NMe_2naphthyl)

Potency. Samples of the 14 new CADA compounds were tested for CD4 down-modulation either in their analytically pure (>95%) free base forms or as hydrochloride salts, as indicated in the Experimental Section for compositions determined by combustion microanalysis. Most of the compounds tested were stoichiometric hydrates of monohydrochloride salts (or dihydrochoride salts when a basic site was present in a side arm). The CD4 down-modulation potencies of the new CADA compounds described in this publication are given in Table 1 as IC_{50} values (concentration producing 50% decrease in CD4 in Chinese hamster ovary/CD4/yellow fluorescent protein (CHO·CD4-YFP) cells after 24 h of drug treatment). Also compared in Table 1 are the CD4 down-modulation potencies of the five structurally related compounds shown in Figure 1, the symmetrical compounds CADA, **1**, and **2**, and unsymmetrical analogues **3** and **4**. Also given for each compound in Table 1 are pIC_{50} values ($-\log_{10} IC_{50}$), which is, in principle, proportional to the negative free energy of binding of the small molecule to its binding site. This is rigorously true if the compounds bind only to the site of CD4 down-modulation or do not distribute differently between various binding sites. Since the IC_{50} values are measured in cell-based assays, different distributions of different compounds between various binding sites is possible. On the other hand, we believe that energetic analysis of the results is still useful, as it may lead to postulation of new compounds for synthesis and testing.

Replacement of the benzyl tail group of CADA with cyclohexylmethyl (**1**) or the tosyl side arms of CADA with 4-methoxybenzenesulfonyl (**2**) was previously found to increase potency for CD4 down-modulation, as shown in Figure 1; the current results in a different cell system reproduce these trends. Thus, it was of interest to compare the effects of different combinations of these substitutions. As seen in Table 1, replacement of both tosyl side arms of CADA with 4-methoxybenzenesulfonyl in addition to replacing the tail with cyclohexylmethyl gives a slight further increase in potency (**10**). The two analogues with single side arm substitutions, **42** with a benzyl tail and **31** with a cyclohexylmethyl tail, were of greater interest to test the proposed, unsymmetrical, two-site binding model shown in Figure 1. The potency of **42** is between those of the symmetrical benzyl tail compounds CADA and **2**, while unsymmetrical cyclohexylmethyl tail analogue **31** is more potent than either symmetrical analogue, **1** or **10**. Compound **31** is the most potent CADA analogue synthesized to date.

Relative to CADA, monodansyl analogues **3** and **4** appear to be less potent than found previously in different cell systems,

dx.doi.org/10.1021/jm2002603 |*J. Med. Chem.* 2011, 54, 5712–5721

Scheme 4

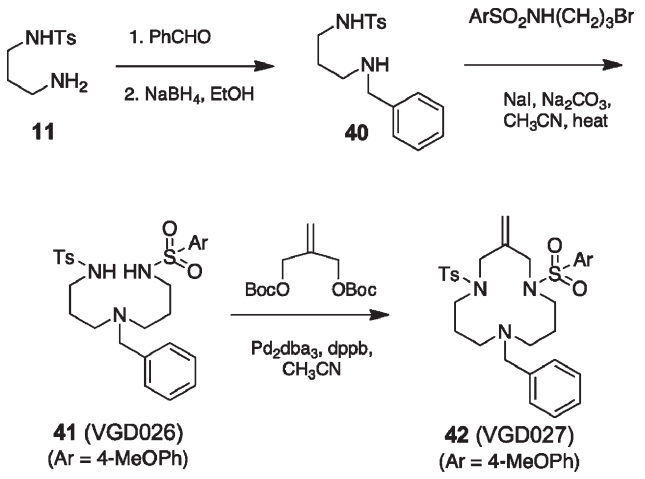

though cyclohexylmethyl tail analogue **4** is still found to be more potent than benzyl tail system **3**. Replacement of the second tosyl side arm of **4** with 4-methoxybenzenesulfonyl further improves potency, making **36** the most potent fluorescent CADA analogue to date. Compound **32**, bearing a naphthalene-1-sulfonyl in place of the dansyl group of **4**, is marginally more potent than **4**, suggesting that the dimethylamino group of the dansyl system does not contribute to binding. The isomer with a naphthalene-2-sulfonyl side arm (**33**) is much more potent than **32** and slightly more potent than ditosyl side arm analogue **1**, suggesting the importance of side arm size and shape. Replacing one of the naphthalene-1-sulfonyl carbons with nitrogen, as in isoquinoline-5-sulfonyl analogue **30**, greatly decreases potency, as does complete removal of one side arm in **39**. Replacement of one tosyl methyl group of **1** with bulky *tert*-butyl in **28** or electronegative nitro in **34** causes nearly 4-fold decreases in activity, while replacement of a methyl with smaller chloro in **29** or with hydrogen in **35** causes more modest decreases in potency. Interestingly, movement of a nitro group from the para position of one benzene side arm in **34** to the ortho position in **37** restores potency almost to the level of **1**.

Additivity. The mechanism by which CADA compounds inhibit cotranslational translocation of CD4 across the ER membrane is not known. It is likely that the biomolecular target is a protein, such as the Sec61 channel,[42] the CD4 signal peptide sequence, or a combination of both. The third possibility is precedented by the mechanism of inhibition of cotranslational translocation of certain proteins in endothelial cells by cotransins[43] and related compounds.[44] Analyzing structure−activity relationships can help to infer molecular characteristics of the drug-binding site, to increase potency, and to develop analogues as tools for elucidating the drug target. A common approach in medicinal chemistry is to consider the contribution of each molecular fragment to the total binding energy of the drug.

Protein−ligand affinity, as described by the binding or association constant K_a (or the inverse, dissociation constant K_d) is determined by the equilibrium free energy ΔG. Free energy is composed of enthalpic (ΔH) and entropic (ΔS) contributions, according to the Gibbs equation, $\Delta G = \Delta H - T\Delta S$. The driving force for association of a small molecule with a protein is thus determined by changes in both enthalpy and entropy. Enthalpic contributions include ligand−protein interactions (e.g., van der Waals, hydrogen bonding, ion−dipole, and dipole−dipole), as well as altered interactions within the protein structure induced by ligand binding. Entropic contributions result from decreased ligand translational and rotational entropy, residual motion of both the ligand and protein in the bound state, and solvent effects, such as increased motion of water molecules released from both the ligand and protein upon binding. It is well recognized that these diverse factors confound simplistic attempts to assess the individual contributions of fragments in drug design.[45,46] Enthalpic contributions of each fragment may be additive, but there is no reason to expect entropic contributions to be additive, according to first principles. A general observation termed "enthalpy/entropy compensation" is that enthalpically favorable interactions often produce opposite entropy effects, resulting in small changes in free energy.[45,46]

Despite the fundamental fallacy of adding group energy increments to obtain binding energies, detection of additive or nonadditive effects may produce useful insights about drug−receptor interactions. For example, Williams proposed that incremental introduction of new binding interactions, or increasing the strength of existing interactions, can be "cooperative" when residual motion of the ligand within the binding site is not further reduced.[45] Thus, the entropic cost of restricting motion (of both the ligand and the protein) has already been paid, and new (or stronger) interactions are less compensated by entropy. There may also be an enthalpic component to this cooperativity

Table 1. CD4 Down-Modulating Activities of CADA Compounds in CHO·CD4-YFP Cells

	IC_{50} (μM)[b]			
compd[a]	mean	±	SDV	pIC_{50}[c]
CADA	0.56	±	0.046	6.25
1	0.19	±	0.003	6.73
2	0.23	±	0.003	6.64
3	5.9	±	3.9	5.23
4	1.06	±	0.063	5.97
28	0.78	±	0.033	6.11
29	0.36	±	0.031	6.44
30	>25			4.64
31	0.046	±	0.002	7.34
32	0.94	±	0.035	6.03
33	0.18	±	0.015	6.75
34	0.76	±	0.033	6.12
35	0.43	±	0.012	6.36
42	0.30	±	0.027	6.53
36	0.73	±	0.050	6.14
37	0.22	±	0.024	6.65
39	19	±	9.3	4.73
10	0.13	±	0.006	6.87

[a] CADA, **1**, and **4** were used as HCl salts, while **2** and **3** were used in their free base forms, as described in ref 30. All VGD compounds were used in their free base or salt forms, as indicated for combustion microanalysis results in the Experimental Section. [b] IC_{50}: inhibitory concentration 50%, i.e., concentration at which 50% down-modulation of CD4 expression was measured in CHO·CD4-YFP after 24 h of drug treatment. Values are the mean + standard deviation from three independent experiments (except for **35**, **37**, and **39**, for which two independent experiments were done). [c] $pIC_{50} = -\log(IC_{50})$.

dx.doi.org/10.1021/jm2002603 |J. Med. Chem. 2011, 54, 5712–5721

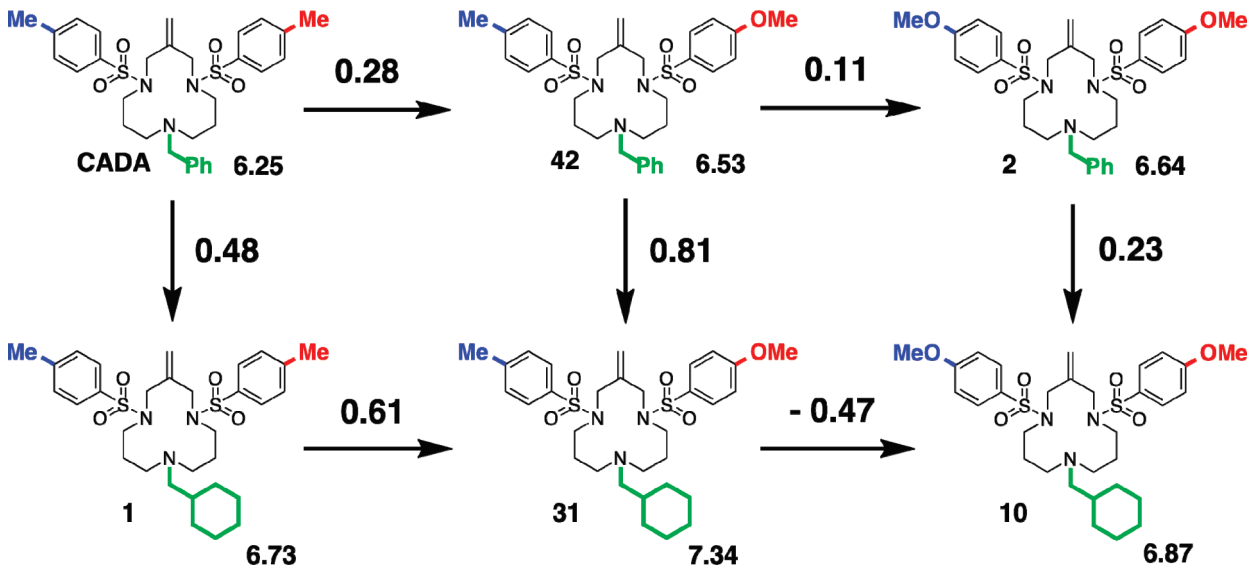

Figure 2. Thermodynamic cycle comparing energy effects of substitutions, starting with CADA (upper left). The pIC_{50} for CD4 down-modulation is given at lower right of each compound structure. Numbers above or beside each arrow represent change in pIC_{50} for each substitution.

in that proteins can become more tightly packed upon ligand binding, a possible explanation for a number of exceedingly strong bimolecular interactions.[47] In this context, positive cooperativity occurs when ligand binding is stronger than the sum of its parts, which is different from the definition of cooperativity used for allosteric interactions in proteins with more than one binding site. A recent thermodynamic and structural study of thrombin inhibitors examining additivity of functional group contributions found that the greatest cooperative interactions were associated with decreasing loss of residual entropy upon introduction of additional interactions (zipper-type mechanism).[48]

In the present study, it was of interest to examine the energetic contributions of substituents in the most potent compound, **31**. The relevant molecular structures and corresponding changes in pIC_{50} values are displayed in the thermodynamic cycle shown in Figure 2. As stated previously, pIC_{50} values are directly proportional to the negative free energy of binding if the compounds bind only to the site of CD4 down-modulation or do not distribute differently between various binding sites. Replacement of one tosyl side arm of CADA by 4-methoxybenzenesulfonyl in **42** increases potency by 0.28 pIC_{50} units, while replacement of the benzyl tail with cyclohexylmethyl in **1** increases potency by 0.48 pIC_{50} units. The same substitutions on **1** and **42** have about double the energetic effect (0.61 and 0.81, respectively). Thus, functional group contributions in the transformation of CADA to **31** are nonadditive and show positive cooperativity. It is tempting to conclude that either substitution on CADA results in most of the loss of residual motion attending binding of **31** to its target. Accordingly, the structure of **31** is very well adapted to fit the binding site and replacement of the second tosyl side arm with 4-methoxybenzenesulfonyl in **10** *decreases* potency by 0.47 pIC_{50} units, possibly because the larger methoxy group fits less well than methyl in the binding site. The same replacement in **42** causes a slight *increase* in potency for **2**, perhaps because the benzyl tail causes a different placement of the side arms in their respective binding sites. The high potency of unsymmetrical compound **31** agrees with the unsymmetrical binding model shown in Figure 1, though it remains to be determined which one of the two different side arms fits into which of the two sites.

From the binding data available in Table 1, it is possible to construct a second thermodynamic cycle, which is shown in Figure 3. For monodansyl compound **3**, replacement of the benzyl tail by cyclohexylmethyl improves potency by 0.74 pIC_{50} units (**4**), whereas changing the dansyl side arm to 4-methoxybenzenesulfonyl causes a greater enhancement (1.30 pIC_{50} units, **42**). The corresponding substitutions on **42** or **4** produce almost the same energetic effects (changes of 0.81 and 1.37, respectively). This differs from the increased effect of the second substitution in either pathway converting CADA to **31** (Figure 2). In Figure 3, the starting structure, **3**, is about 10-fold less potent than CADA; hence, its molecular structure is more poorly adapted to the binding site and a large degree of residual motion is expected in the complex. Replacement of the benzyl tail by cyclohexylmethyl would not be expected to greatly reduce residual motion, but changing dansyl to 4-methoxybenzenesulfonyl should. These expected differences in residual motion changes might account for the apparent lack of cooperativity in this case. Of course, the presence of the dimethylamino group in dansyl introduces the possibility of solvent-related entropy changes not associated with motion in the drug−protein complex. Finally, replacement of the tosyl side arm of **4** with 4-methoxybenzenesulfonyl causes a modest increase in potency for **36**, as seen for the same substitution in **42** (Figure 2).

Symmetry. The molecular structures of many drugs are symmetrical, as defined by symmetry elements including rotational axes, mirror planes, or centers of inversion.[49−53] In many cases, drug symmetry may reflect the method of synthesis because it is often easier to synthesize symmetrical structures, as is the case with CADA compounds. While amino acids, nucleotides, and carbohydrates are asymmetric (chiral), in rare cases the drug-binding site may be dissymmetric and possess rotational symmetry, for example, in multimeric protein assemblies that often occur in viruses.[53] The binding site for CADA compounds, which probably involves the Sec 61 translocon, the CD4 signal peptide sequence, or both, is unlikely to be symmetric. Therefore, it is understandable that unsymmetrical compound **31** is more potent than either of its symmetrical analogues, **1** or **10** (cf. Figure 2). The slightly greater potency of symmetrical

dx.doi.org/10.1021/jm2002603 |*J. Med. Chem.* 2011, 54, 5712–5721

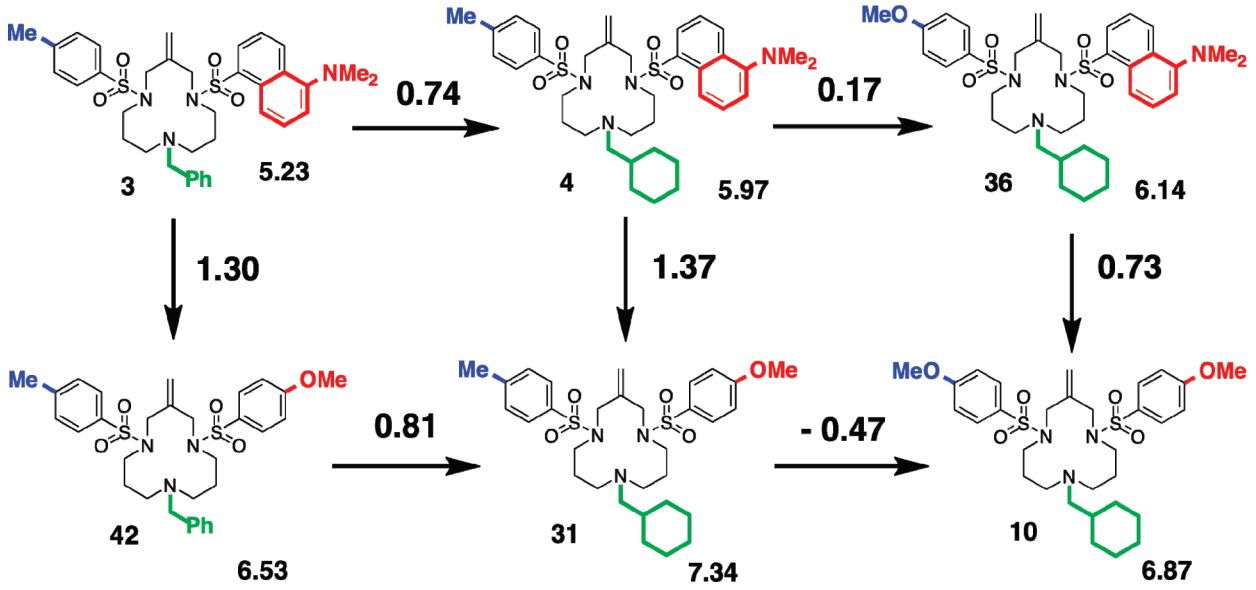

Figure 3. Thermodynamic cycle comparing energy effects of substitutions, starting with **3** (upper left). The pIC_{50} for CD4 down-modulation is given at lower right of each compound structure. Numbers above or beside each arrow represent change in pIC_{50} for each substitution.

2 over unsymmetrical **42**, however, suggests that symmetry is not necessarily more important than the physicochemical properties of substituents. As stated previously, potencies were measured in whole cell assays, and some observed differences might also arise from different distribution of the compounds between more than one potential binding site. Compound **31** is the most potent CADA compound to date, and its potency is consistent with unsymmetrical binding models, such as that displayed in Figure 1. Its discovery paves the way for future, conformationally controlled analogues capable of separately probing the characteristics of the two different side arm binding sites.

CONCLUSIONS

Effective methods have been developed for the synthesis of diverse, unsymmetrical CADA compounds. CD4 down-modulation assays of the 14 new compounds displayed a wide range of potency and revealed the most potent CADA compound discovered to date, **31**, and the most potent fluorescent analogue, **36**. Relative to CADA, group contributions to the potency of **31** are nonadditive and show positive cooperativity, consistent with the zipper-type mechanism in which additional binding interactions exact lower entropy costs due to smaller changes in residual motion. This conclusion is based on the assumption that the potencies of these compounds are directly related to their affinity for the CD4 down-modulation binding site. Compound **31** is more potent than either of its symmetrical analogues, consistent with the proposed, unsymmetrical binding model. These results lay important groundwork for developing effective tools for elucidating the exact molecular mechanism by which CADA compounds inhibit cotranslational translocation of nascent CD4. Discovery of this mechanism could pave the way to designing drugs for inhibiting expression of other membrane proteins.

EXPERIMENTAL SECTION

Flow Cytometry. To study the effect of CADA on CD4 expression, CHO cells, stably expressing CD4-YFP (huCD4 fused at its COOH-terminus to the yellow fluorescent protein [YFP]), were treated for 24 h with different concentrations of CADA or its analogues at 37 °C. Cells were then washed, fixed in 1% formaldehyde, and analyzed immediately. Data were acquired with a FACSCalibur flow cytometer (BD Biosciences) using the 488 nm laser line and CellQuest software (BD Biosciences). YFP was measured with the FL-1 detector, and data were analyzed with FLOWJO software (Tree Star, San Carlos, CA). Down-modulation of CD4 was evaluated by the decrease in fluorescence intensity on CADA-treated cells relative to matched, untreated cells. To calculate the efficiency of CD4 down-modulation, the median fluorescence intensity (MFI) for YFP for each sample was expressed as a percentage of the MFI of control cells (after subtracting the background MFI of the nontransfected control cells).

General Methods. All reactions were performed under an atmosphere of dry nitrogen. Reagents and solvents purchased from Aldrich Chemical Co., Acros Organics, or Fisher Scientific were of ACS reagent grade or better and were used without purification, unless indicated otherwise. Anhydrous acetonitrile was distilled from CaH_2. HCl (2 N) in methanol/water was prepared from 42 mL of concentrated aqueous HCl (12.1 N) and 210 mL of methanol. For macrocyclization reactions, the disulfonamide intermediate (previously washed with aqueous NaOH, as described for deprotonation of HCl salts) and 2-methylene 1,3-propanebis(*tert*-butylcarbonate) were dried in vacuo for at least 16 h and then dissolved in anhydrous acetonitrile with 1,4-bis(diphenylphosphino)butane (dppb), and $Pd_2(dba)_3$ was added last. Column chromatography was performed with Sorbent Technologies neutral alumina (50−200 μm) or Sorbent Technologies standard grade silica (32−63 μm), unless noted otherwise. Melting points were measured on Thomas-Hoover or Mel-Temp apparatus and are uncorrected. ^{1}H NMR (400 or 500 MHz) and ^{13}C NMR (100 or 125 MHz) spectra were acquired on a Varian 400 or Varian Unity +500 spectrometer. All chemical shifts (δ) are reported in ppm units relative to solvent resonances, as follows: ^{1}H, $CDCl_3$/TMS = 0.00, DMSO-d_6 = 2.50, CD_3OD = 3.31; ^{13}C, $CDCl_3$ = 77.23, DMSO-d_6 = 39.7, CD_3OD = 49.15. Infrared spectra (IR) were recorded on a Nicolet 6700 FTIR spectrometer. Mass spectra (MS) were acquired on a Waters Micromass ZQ electrospray ionization quadrupole mass spectrometer with positive ion detection (capillary voltage of 3.5 kV). High-resolution mass spectra (HRMS) were acquired on an Agilent 6230 TOF mass spectrometer. Samples for elemental analysis were dried at 78 °C (0.1 mm) for 2 days,

dx.doi.org/10.1021/jm2002603 |*J. Med. Chem.* 2011, 54, 5712–5721

unless stated otherwise, and microanalysis was performed by NuMega Resonance Labs, Inc. Samples tested for CD4 down-modulation were greater than 95% pure, as shown by combustion microanalysis.

9-Cyclohexylmethyl-1,5-(4-methoxybenzenesulfonyl)-3-methylene-1,5,9-triazacyclododecane (10). A solution of 0.21 g (0.39 mmol) of 3-methylene-1,5-bis(4-methoxybenzenesulfonyl)-1,5,9-triazacyclododecane (**9**) and 0.29 g (2.6 mmol) of cyclohexanecarboxaldehyde in 10 mL of absolute ethanol was stirred at room temperature for 1 h. Then a solution of 87 mg (1.4 mmol) of $NaBH_3CN$ in 5 mL of absolute ethanol was added dropwise over 10 min. The resulting mixture was stirred at room temperature for 24 h and then concentrated to dryness by rotary evaporation. A solution of the residue in 10 mL of CH_2Cl_2 was washed with H_2O (3 × 5 mL) followed by 5 mL of saturated aqueous NaCl, then dried (Na_2SO_4). Concentration by rotary evaporation followed by two silica column chromatograms, eluting with CH_2Cl_2/MeOH, gave 0.17 g (71%) of **10** as a colorless, viscous oil. ^{1}H NMR (500 MHz, $CDCl_3$/TMS) δ 7.72 (m, 4 H, *o*-$ArSO_2$), 7.00 (m, 4 H, *m*-$ArSO_2$), 5.18 (s, 2 H, C=CH_2), 3.88 (s, 6 H, OCH_3), 3.79 (s, 4 H, H2, H4), 3.15 (t, 7 Hz, 4 H, H6, H12), 2.27 (t, 6 Hz, 4 H, H8, H10), 1.97 (d, 7 Hz, 2 H, CH_2Cy), 1.62 (m, 10 H, H7, H11, Cy), 1.25 (m, 1 H, Cy), 1.14 (m, 2 H, Cy), 0.70 (m, 2 H, Cy). ^{13}C NMR (125 MHz, $CDCl_3$) δ 163.1, 138.2, 130.5, 129.5, 116.7, 114.5, 62.4, 55.8, 51.1, 50.6, 44.3, 36.1, 32.1, 27.0, 26.2, 24.7. IR (neat, cm^{-1}) 2923 (w), 2848 (w), 2801 (w), 1596 (m), 1578 (w), 1497 (m), 1462 (w), 1334 (m), 1306 (m), 1258 (s), 1153 (s), 1092 (m), 1026 (m), 938 (m), 910 (m), 834 (m), 806 (m), 729 (s), 690 (m).

***10*·*HCl*.** A solution of 0.13 g of **10** in 10 mL of 2 N HCl in methanol/water was stirred at room temperature for 4 h. Concentration by rotary evaporation and drying (0.1 mm) gave a residue that was triturated with ether (5 × 10 mL) using sonication and dried in vacuo, giving 0.13 g (93%) of **10**·HCl as a white powder. ^{1}H NMR (500 MHz, $CDCl_3$/TMS) δ 7.69 (m, 4 H, *o*-$ArSO_2$), 7.02 (m, 4 H, *m*-$ArSO_2$), 5.34 (s, 2 H, C=CH_2), 3.90 (s, 6 H, $ArOCH_3$), 3.70 (m, 4 H, H2, H4), 3.40 (m, 2 H, H8/H10), 3.19 (m, 4 H, H6/H8/H10/H12), 3.12 (m, 2 H, H6/H12), 2.77 (t, 7 Hz, 2 H, CH_2Cy), 2.32 (m, 2 H, H7/H11), 1.97 (m, 4 H, H7/H11, Cy), 1.80 (m, 3 H, Cy), 1.69 (m, 1 H, Cy), 1.2 (m, 5 H, Cy). IR (neat, cm^{-1}) 3401 (w), 2930 (w), 2851 (w), 1596 (m), 1577 (w), 1498 (m), 1455 (w), 1336 (m), 1307 (w), 1262 (m), 1157 (s), 1092 (m), 1023 (w), 806 (w). MS *m*/*z* 620 (MH^+). Anal. Calcd for $C_{31}H_{45}N_3O_6S_2$·HCl: C, 56.73; H, 7.06; N, 6.40. Found: C, 56.92; H, 7.46; N, 6.52.

***N*-(3-Aminopropyl)-*p*-toluenesulfonamide (11).** A filtered solution of 50.4 g (0.26 mol) of *p*-toluenesulfonyl chloride in 180 mL of toluene was added dropwise over 6 h to a vigorously stirred solution of 65 mL (58 g, 0.78 mol) of 1,3-diaminopropane and 80 mL of toluene. The resulting white suspension was stirred at room temperature overnight (12−17 h). The white precipitate was collected by vacuum filtration, washed with 20 mL of cold toluene, and dried (0.1 mm) overnight, yielding 67 g of crude product as a white solid, mp 95−135 °C. This solid was stirred for approximately 0.5 h with 1 L of 1:1 (v/v) methanol/water. Then the resulting suspension was filtered (vacuum). The residue consisted of 4.08 g of 1,3-bis(*p*-toluenesulfonamido)propane, mp 140−147 °C (lit.[38] 147−149 °C). The filtrate was stored at 4 °C for 3 h, then filtered to give an additional 0.43 g of 1,3-bis(*p*-toluenesulfonamido)propane, mp 143−146 °C. The filtrate was concentrated by boiling to a volume of about 600 mL, then stored at 4 °C for 3 h. The resulting precipitate was collected by vacuum filtration, washed with water, and dried (0.1 mm). The filtrate was stored at 4 °C for 3 h and filtered to obtain a second crop. A total yield of 28.7 g (48%) of **11** was obtained as beige crystals, mp 114−117 °C (lit. 112−114 °C,[39] 113−115 °C[38]). ^{1}H NMR (400 MHz, CD_3OD) δ 7.73 (m, 2 H, *o*-Ts), 7.38 (m, 2 H, *m*-Ts), 2.88 (t, 7 Hz, 2 H, CH_2NH), 2.63 (t, 7 Hz, 2 H, CH_2NH_2), 2.42 (s, 3H, $ArCH_3$), 1.59 (quint, 7 Hz, 2 H, CCH_2C). ^{13}C NMR (125 MHz, CD_3OD) δ 144.7, 139.0, 130.9, 128.2, 41.7, 39.7, 33.5, 21.6.

***N*-(3-*p*-Toluenesulfonamidopropyl)benzylamine (40).** A mixture of 2.01 g (8.80 mmol) of *N*-(3-aminopropyl)-*p*-toluenesulfonamide (**11**), 1.05 g (9.86 mmol) of benzaldehyde, 3.18 g (26.4 mmol) of anhydrous $MgSO_4$, and 25 mL of CH_2Cl_2 was stirred at room temperature for 24 h and then filtered under vacuum through a fine porosity sintered glass funnel. The white residue was washed with 10 mL of CH_2Cl_2. The combined filtrates were concentrated by rotary evaporation, and the resulting colorless oil was dried in vacuo. A solution of the residue in 10 mL of absolute ethanol was stirred under nitrogen as 0.45 g (12 mmol) of $NaBH_4$ was added in portions over 30 min. The reaction mixture was stirred at room temperature overnight (at least 12 h), then was vacuum filtered through a medium porosity sintered glass funnel, rinsing the reaction flask and the residue with ∼10 mL of ethanol. The combined filtrates were concentrated to dryness by rotary evaporation, and the residue was stirred with 20 mL of water. The resulting, slightly cloudy mixture was extracted with CH_2Cl_2 (3 × 10 mL). The combined CH_2Cl_2 extracts were dried (Na_2SO_4) and concentrated by rotary evaporation, yielding 1.97 g (70%) of **40** as a white solid. ^{1}H NMR (500 MHz, $CDCl_3$/TMS) δ 7.71 (m, 2 H, *o*-Ts), 7.32 (m, 2 H, *o*-Ph), 7.26 (m, 5 H, *m*,*p*-Ph, *m*-Ts), 3.70 (s, 2 H, CH_2Ph), 3.04 (t, 6 Hz, 2 H, CH_2NH), 2.67 (t, 6 Hz, 2 H, CH_2N), 2.41 (s, 3 H, $ArCH_3$), 1.62 (quint, 6 Hz, 2 H, CCH_2C). ^{13}C NMR (125 MHz, $CDCl_3$) δ 143.2, 139.8, 137.3, 129.8, 128.7, 128.3, 127.3, 127.2, 54.0, 48.5, 43.8, 28.0, 21.7. IR (neat, cm^{-1}) 3043 (w), 2831 (w), 1598 (w), 1495 (w), 1477 (w), 1454 (w), 1324 (s), 1304 (m), 1286 (w), 1273 (w), 1185 (w), 1155 (s), 1089 (m), 1072 (s), 1043 (w), 1031 (w), 979 (m), 835 (m), 815 (s), 781 (m), 742 (s), 702 (s), 660 (s). MS *m*/*z* 319 (MH^+). Anal. Calcd for $C_{17}H_{24}N_2O_4S$: C, 63.72; H, 7.55; N, 8.74. Found: C, 63.78; H, 6.94; N, 8.85.

***N*-(4-Methoxybenzenesulfonyl)-*N*′-(*p*-toluenesulfonyl)bis-(3-aminopropyl)benzylamine (41).** A mixture of 0.80 g (2.5 mmol) of **40**, 0.40 g (3.8 mmol) of Na_2CO_3, 0.18 g (1.2 mmol) of NaI, 0.93 g (3.0 mmol) of *N*-(3-bromopropyl)-4-methoxybenzenesulfonamide, and 9 mL of MeCN was stirred with heating under reflux for 24 h, then cooled to room temperature and filtered through a fine porosity sintered glass funnel, washing the residue with 10 mL of MeCN. The combined filtrates were concentrated by rotary evaporation, and a solution of the resulting residue in 15 mL of CH_2Cl_2 was washed with 3 × 5 mL of H_2O, dried (Na_2SO_4), and concentrated by rotary evaporation. The resulting faintly yellow oil was dried in vacuo to give 1.34 g (98%) of **41**. Alumina column chromatography, eluting with CH_2Cl_2/EtOAc, gave 0.75 g (54%) of **41** as an amber viscous oil. ^{1}H NMR (500 MHz, $CDCl_3$/TMS) δ 7.76 (m, 2 H, *o*-$ArSO_2$), 7.70 (m, 2 H, *o*-Ts), 7.27 (m, 5 H, *o*, *p*-Ph, *m*-Ts), 7.20 (m, 2 H, *m*-Ph), 6.96 (m, 2 H, *m*-$ArSO_2$), 3.86 (s, 3 H, $ArOCH_3$), 3.46 (s, 2 H, CH_2Ph), 2.92 (m, 4 H, CH_2NH), 2.43 (t, 6 Hz, 4 H, CH_2N), 2.42 (s, 3 H, $ArCH_3$), 1.65 (quint, 6 Hz, 4 H, CCH_2C). ^{13}C NMR (125 MHz, $CDCl_3$) δ 163.0, 143.4, 138.1, 137.2, 131.7, 129.9, 129.41, 129.35, 128.7, 127.6, 127.3, 114.4, 58.9, 55.8, 52.1, 42.40, 42.38, 26.2, 21.7. IR (neat, cm^{-1}) 3279 (w), 2946 (w), 1597 (m), 1579 (w), 1497 (m), 1453 (w), 1324 (m), 1260 (m), 1155 (s), 1094 (m), 1026 (w), 962 (w), 910 (w), 835 (m), 816 (w), 736 (m), 700 (w), 665 (m).

***41*·*HCl*.** A solution of 0.13 g of **41** in 10 mL of 2 N HCl in methanol/water was stirred at room temperature for 4 h then concentrated by rotary evaporation. The residue was dried (0.1 mm), then triturated with ether (5 × 10 mL) using sonication, giving 0.12 g (86%) of **41**·HCl as a beige powder. ^{1}H NMR (500 MHz, CD_3OD) δ 7.78 (m, 2 H, *o*-$ArSO_2$), 7.73 (m, 2 H, *o*-Ts), 7.52 (m, 5 H, Ph), 7.40 (m, 2 H, *m*-Ts), 7.09 (m, 2 H, *m*-$ArSO_2$), 4.36 (s, 2 H, CH_2Ph), 3.87 (s, 3 H, $ArOCH_3$), 3.22 (m, 4 H, CH_2N^+), 2.91 (m, 4 H, CH_2NH), 2.43 (s, 3 H, $ArCH_3$), 1.96 (m, 4 H, CCH_2C). IR (neat, cm^{-1}) 3075 (w), 2933 (w), 2844 (w), 1596 (w), 1499 (w), 1322 (m), 1260 (m), 1156 (s), 1091 (m), 1027 (w), 926 (w), 831 (m), 806 (m), 755 (m), 734 (m), 704 (m), 689 (m). MS *m*/*z* 546 (MH^+). Anal. Calcd for $C_{27}H_{35}N_3O_5S_2$·HCl·H_2O: C, 54.03; H, 6.38; N, 7.00. Found: C, 54.16; H, 6.71; N, 7.17.

9-Benzyl-1-(4-methoxybenzenesulfonyl)-3-methylene-5-(*p*-toluenesulfonyl)-1,5,9-triazacyclododecane (42). A mixture of

0.30 g (0.55 mmol) of **42**, 0.40 g (1.4 mmol) of 2-methylene 1,3-propanebis(*tert*-butylcarbonate), 15 mg (0.034 mmol) of dppb, 16 mg (0.017 mmol) of tris(dibenzylideneacetone)dipalladium(0), and 35 mL of anhydrous MeCN was stirred and heated under reflux for 24 h, cooled to room temperature, and concentrated to dryness by rotary evaporation. A solution of the residue in 26 mL of CH_2Cl_2 was washed with saturated aqueous $NaHCO_3$ (2 × 9 mL) and saturated aqueous NaCl (9 mL), dried (Na_2SO_4), and concentrated to dryness by rotary evaporation. **42**·HCl. A solution of crude **42** in 10 mL of 2 N HCl in methanol/water was stirred at room temperature for 4 h, then concentrated by rotary evaporation. The residue was dried (0.1 mm), then triturated with ether (5 × 15 mL) using sonication, giving 0.33 g (92%) of **42**·HCl as a cream-colored powder. **42**·HCl was further purified by adding ether dropwise to a solution in CH_2Cl_2 until cloudiness was observed. The precipitated solid was collected by filtration and dried in vacuo, giving 0.20 g (56%) of **42**·HCl·H_2O as a cream-colored solid. ^{1}H NMR (500 MHz, CD_3OD) δ 7.75 (m, 2 H, *o*-$ArSO_2$), 7.70 (m, 2 H, *o*-Ts), 7.55 (m, 5 H, Ph), 7.46 (m, 2 H, *m*-Ts), 7.14 (m, 2 H, *m*-$ArSO_2$), 5.41 (s, 1 H, C=CH_2), 5.40 (s, 1 H, C=CH_2), 4.38 (s, 2 H, CH_2Ph), 3.90 (s, 3 H, $ArOCH_3$), 3.76 (s, 4 H, H2, H4), 3.45 (bs, 2 H, H8/H10), 3.35 (bs, 2 H, H8/H10), 3.19 (m, 4 H, H6, H12), 2.46 (s, 3 H, $ArCH_3$), 2.06 (bs, 4 H, H7, H11). IR (neat, cm^{-1}) 2923 (w), 2395 (w), 1596 (w), 1498 (w), 1457 (w), 1333 (m), 1306 (m), 1261 (m), 1154 (s), 1106 (m), 1091 (m), 1020 (m), 924 (w), 897 (m), 835 (m), 806 (s), 783 (m), 736 (s), 686 (s). MS *m*/*z* 598 (MH^+). Anal. Calcd for $C_{31}H_{39}N_3O_5S_2$·HCl·H_2O: C, 57.08; H, 6.49; N, 6.44. Found: C, 57.31; H, 6.84; N, 6.40.

■ ASSOCIATED CONTENT

Supporting Information. Detailed synthetic procedures and characterization data (^{1}H and ^{13}C NMR, IR, MS, and combustion microanalysis) for compounds **12**−**39**. This material is available free of charge via the Internet at http://pubs.acs.org.

■ AUTHOR INFORMATION

Corresponding Author

*Phone: 775-784-1842. Fax: 775-784-6804. E-mail: twb@unr.edu.

■ ACKNOWLEDGMENT

This work was supported by the K.U. Leuven (GOA No. 10/014 and No. PF/10/018), the FWO (No. G.485.08), the CHAARM Project of the European Commission, and the Dormeur Investment Service Ltd. We are grateful to B. Provinciael, S. Claes, and E. Fonteyn for excellent technical assistance. Funding from the National Science Foundation (Grnat CHE-0521191) in support of NMR spectrometers in the Department of Chemistry, University of Nevada, is also gratefully acknowledged.

■ ABBREVIATIONS USED

ACE-Cl, α-chloroethyl chloroformate; AIDS, acquired immune deficiency syndrome; CADA, cyclotriazadisulfonamide; CD4, cluster of differentiation 4; dan, 5-dimethylaminonaphthalene-1-yl; dppb, 1,4-bis(diphenylphosphino)butane; CHO·CD4-YFP, Chinese hamster ovary/CD4/yellow fluorescent protein; ER, endoplasmic reticulum; HIV, human immunodeficiency virus; SIV, simian immunodeficiency virus

■ REFERENCES

(1) Littman, D. R. The structure of the CD4 and CD8 genes. *Annu. Rev. Immunol.* **1987**, *5*, 561–584.

(2) Janeway, C. A., Jr. The role of CD4 in T-cell activation: accessory molecule or co-receptor? *Immunol. Today* **1989**, *10*, 234–238.

(3) Ellmeier, W.; Sawada, S.; Littman, D. R. The regulation of CD4 and CD8 coreceptor gene expression during T cell development. *Annu. Rev. Immunol.* **1999**, *17*, 523–554.

(4) Nepom, G. T. Therapy of autoimmune diseases: clinical trials and new biologics. *Curr. Opin. Immunol.* **2002**, *14*, 812–815.

(5) Taylor, P. C. Antibody therapy for rheumatoid arthritis. *Curr. Opin. Pharmacol.* **2003**, *3*, 323–328.

(6) Liu, E.; Moriyama, H.; Paronen, J.; Abiru, N.; Miao, D.; Yu, L.; Taylor, R. M.; Eisenbarth, G. S. Nondepleting anti-CD4 monoclonal antibody prevents diabetes and blocks induction of insulin autoantibodies following insulin peptide B:9-23 immunization in the NOD mouse. *J. Autoimmun.* **2003**, *21*, 213–219.

(7) Hanns-Martin, L. T-cell-activation inhibitors in rheumatoid arthritis. *BioDrugs* **2003**, *17*, 263–270.

(8) Kim, Y. H.; Douvic, M.; Obitz, E.; Gniadecki, R.; Iversen, L.; Osterborg, A.; Whittaker, S.; Illidge, T. M.; Schwarz, T.; Kaufmann, R.; Cooper, K.; Knudsen, K. M.; Lisby, S.; Baadsgaard, O.; Knox, S. J. Clinical efficacy of zanolimumab (HuMax-CD4): two phase 2 studies in refractory cutaneous T-cell lymphoma. *Blood* **2007**, *109* (11), 4655–4662.

(9) Dalgleish, A. G.; Beverly, P. C.; Clapham, P. R.; Crawford, D. H.; Greaves, M. F.; Weiss, R. A. The CD4 (T4) antigen is an essential component of the receptor for the AIDS retrovirus. *Nature* **1984**, *312*, 763–767.

(10) Klatzmann, D.; Champagne, E.; Chamaret, S.; Gruest, J.; Guetard, D.; Hercend, T.; Gluckman, J. C.; Montagnier, L. T-lymphocyte T4 molecule behaves as the receptor for human retrovirus LAV. *Nature* **1984**, *312*, 767–768.

(11) Freeman, M. M.; Seaman, M. S.; Rits-Volloch, S.; Hong, X.; Kao, C. Y.; Ho, D. D.; Chen, B. Crystal structure of HIV-1 primary receptor CD4 in complex with a potent antiviral antibody. *Structure* **2010**, *18* (12), 1632–1641.

(12) Matthias, L. J.; Azimi, I.; Tabrett, C. A.; Hogg, P. J. Reduced monomeric CD4 is the preferred receptor for HIV. *J. Biol. Chem.* **2010**, *285* (52), 40793–40799.

(13) Veiga, A. S.; Santos, N. C.; Castanho, M. A. R. B. An insight on the leading HIV entry inhibitors. *Recent Pat. Anti-Infect. Drug Discovery* **2006**, *1*, 67–73.

(14) Esté, J. A.; Telenti, A. HIV entry inhibitors. *Lancet* **2007**, *370*, 319–328.

(15) DeClercq, E. The design of drugs for HIV and HCV. *Nat. Rev. Drug Discovery* **2007**, *6*, 1001–1018.

(16) Qian, K.; Morris-Natschke, S. L.; Lee, K.-H. HIV entry inhibitors and their potential in HIV Therapy. *Med. Res. Rev.* **2008**, *2009* (29), 369–393.

(17) Reimann, K. A.; Khunkhun, R.; Lin, W.; Gordon, W.; Fung, M. A humanized, nondepleting anti-CD4 antibody that blocks virus entry inhibits virus replication in rhesus monkeys chronically infected with simian immunodeficiency virus. *AIDS Res. Hum. Retroviruses* **2002**, *18*, 747–755.

(18) Kuritzkes, D. R.; Jacobsen, J.; Powderly, W. G.; Godofsky, E.; DeJesus, E.; Haas, F.; Reimann, K. A.; Larson, J. L.; Yarbough, P. O.; Curt, V.; Shanahan, W. R., Jr. Antiretroviral activity of the anti-CD4 monoclonal antibody TNX-355 in patients infected with HIV type 1. *J. Infect. Dis.* **2004**, *189*, 286–291.

(19) Schols, D. HIV co-receptors as targets for antiviral therapy. *Curr. Top. Med. Chem.* **2004**, *4*, 883–893.

(20) Kazmierski, W. M.; Gudmundsson, K. S.; Piscitelli, S. C. Small Molecule CCR5 and CXCR4-Based Viral Entry Inhibitors for Anti-HIV Therapy Currently in Development. In *Annual Reports in Medicinal Chemistry*; Macor, J. E., Ed.; Academic Press: Amsterdam, 2007; Vol. 42, pp 301−320.

(21) Conti, L.; Varano, B.; Gauzzi, M. C.; Matarrese, P.; Federico, M.; Malorni, W.; Belardelli, F.; Gessani, S. Impairment of human immunodeficiency virus type 1 (HIV-1) entry into Jurkat T cells by constitutive expression of the HIV-1 vpr protein: role of CD4 down-modulation. *J. Virol.* **2000**, *74*, 10207–10211.

(22) Nokta, M. A.; Li, X. D.; Nichols, J.; Mallen, M.; Pou, A.; Asmuth, D.; Pollard, R. B. Chemokine/CD4 receptor density ratios correlate with HIV replication in lymph node and peripheral blood of HIV-infected individuals. *AIDS Res. Hum. Retroviruses* **2001**, *15*, 161–169.

(23) Xiang, J.; McLinden, J. H.; Rydze, R. A.; Chang, Q.; Kaufman, T. M.; Klinzman, D.; Stapleton, J. T. Viruses within the flaviviridae decrease CD4 expression and inhibit HIV replication in human CD4+ cells. *J. Immunol.* **2009**, *183*, 7860–7869.

(24) Lisco, A.; Grivel, J. C.; Biancotto, A.; Vanpouille, C.; Origgi, F.; Malnati, M. S.; Schols, D.; Lusso, P.; Margolis, L. B. Viral interactions in human lymphoid tissue: human herpesvirus 7 suppresses the replication of CCR5-tropic human immunodeficiency virus type 1 via CD4 modulation. *J. Virol.* **2007**, *81*, 708–717.

(25) Vermeire, K.; Bell, T. W.; Choi, H. J.; Jin, Q.; Samala, M. F.; Sodoma, A.; De Clercq, E.; Schols, D. The anti-HIV potency of cyclotriazadisulfonamide analogs is directly correlated with their ability to down-modulate the CD4 receptor. *Mol. Pharmacol.* **2003**, *63*, 203–210.

(26) Beaumier, C. M.; Harris, L. D.; Goldstein, S.; Klatt, N. R.; Whitted, S.; McGinty, J.; Apetrei, C.; Pandrea, I.; Hirsch, V. M.; Brenchley, J. M. CD4 downregulation by memory CD4+ T cells in vivo renders African green monkeys resistant to progressive SIVagm infection. *Nat. Med.* **2009**, *15*, 879–885.

(27) Vermeire, K.; Zhang, Y.; Princen, K.; Hatse, S.; Samala, M.; Dey, K.; Choi, H.-J.; Ahn, Y.; Sodoma, A.; Snoeck, R.; Andrei, G.; De Clercq, E.; Bell, T. W.; Schols, D. CADA inhibits human immunodeficiency virus and human herpesvirus 7 replication by down-modulation of the cellular CD4 receptor. *Virology* **2002**, *302*, 342–353.

(28) Vermeire, K.; Princen, K.; Hatse, S.; De Clercq, E.; Dey, K.; Bell, T. W.; Schols, D. CADA, a novel CD4-targeted HIV inhibitor, is synergistic with various anti-HIV drugs in vitro. *AIDS Res. Hum. Retroviruses* **2004**, *18*, 2115–2125.

(29) Vermeire, K.; Schols, D.; Bell, T. W.; Marsh, M. A small-molecule inhibitor of CD4 protein translocation down-modulates the primary HIV receptor. Manuscript under revision.

(30) Bell, T. W.; Anugu, S.; Bailey, P.; Catalano, V. J.; Dey, K.; Drew, M. G.; Duffy, N. H.; Jin, Q.; Samala, M. F.; Sodoma, A.; Welch, W. H.; Schols, D.; Vermeire, K. Synthesis and structure−activity relationship studies of CD4 down-modulating cyclotriazadisulfonamide (CADA) analogues. *J. Med. Chem.* **2006**, *49*, 1291–1312.

(31) Vermeire, K.; Lisco, A.; Grivel, J.-C.; Scarbrough, E.; Dey, K.; Duffy, N.; Margolis, L.; Bell, T. W.; Schols, D. Design and cellular kinetics of dansyl-labeled CADA derivatives with anti-HIV and CD4 receptor down-modulating activity. *Biochem. Pharmacol.* **2007**, *74*, 566–578.

(32) Richman, J.; Atkins, T. J. Nitrogen analogs of crown ethers. *J. Am. Chem. Soc.* **1974**, *96*, 2268–2270.

(33) Atkins, T. J.; Richman, J. E.; Oettle, W. F. *Macrocyclic Polyamines: 1,4,7,10,13,16-Hexaazacyclooctadecane.*; Wiley: New York, 1988; pp 652−662.

(34) Ali, R.; Anugu, S.; Khan, C.; Demillo, V. G.; Goulinet-Mateo, F.; Lamprecht, K.; Scarbrough, E.; Bell, T. W. Palladium-catalyzed synthesis of 1,5,9-triazacyclododecanes by macrocyclization of disulfonamides with carbonate esters of 2-methylene-1,3-dihydroxypropane. Manuscript in preparation.

(35) Olofsen, R. A.; Abott, D. E. Tests of a piperidino mask for the protection of functionalized carbon sites in multistep syntheses. *J. Org. Chem.* **1984**, *49*, 2795–2799.

(36) Olofsen, R. A.; Martz., J. T.; Senet, J.-P.; Piteau, M.; Malfroot, T. A new reagent for the selective, high-yield N-dealkylation of tertiary amines: improved synthesis of naltrexone and nalbuphine. *J. Org. Chem.* **1984**, *49*, 2081–2082.

(37) Demillo, V. Unsymmetrical Cyclotriazadisulfonamide (CADA) Compounds: Synthesis and CD4 Down-Modulation Potency. Ph.D. Dissertation, University of Nevada, Reno, NV, 2011.

(38) Pokhvisneva, G. V.; Luk'yanov, O. A. Synthesis of 2-substituted 1-tosyl-3(1-tosyliminoalkyl)imidazolidines and hexahydropyrimidines. *Russ. Chem. Bull., Int. Ed.* **2006**, *55*, 903–906.

(39) Antonopoulou, G.; Magrioti, V.; Stephens, D.; Constantinou-Kokotou, V.; Dennis, E. A.; Kokotos, G. Synthesis of 2-oxoamides based on sulfonamide analogs of γ-amino acids and their activity on phospholipase A2. *J. Pept. Sci.* **2008**, *14*, 1111–1120.

(40) Saab, N. H.; West, E. E.; Bieszk, N. C.; Prews, C. V.; Mank, A. R.; Casero, R. A., Jr.; Woster, P. M. Synthesis and evaluation of unsymmetrically substituted polyamine analogues as modulators of human spermidine/spermine-*N*-acetyltransferase (SSAT) and as potential antitumor agents. *J. Med. Chem.* **1993**, *36*, 2998–3004.

(41) Yokoshima, S.; Ueda, T.; Kobayashi, S.; Sato, A.; Kuboyama, T.; Tokuyama, H.; Fukuyama, T. Stereocontrolled total synthesis of (+)-vinblastine. *J. Am. Chem. Soc.* **2002**, *124*, 2137–2139.

(42) Osborne, A. R.; Rapoport, T. A.; van den Berg, B. Protein translocation by the Sec61/SecY channel. *Annu. Rev. Cell Dev. Biol.* **2005**, No. 21, 529–550.

(43) Garrison, J. L.; Kunkel, E. J.; Hegde, R. S.; Taunton, J. A substrate-specific inhibitor of protein translocation into the endoplasmic reticulum. *Nature* **2005**, *436*, 287–289.

(44) Besemer, J.; Harant, H.; Wang, S.; Oberhauser, B.; Marquardt, K.; Foster, C. A.; Schreiner, E. P.; de Vries, J. E.; Dascher-Nadel, C.; Lindley, I. J. D. Selective inhibition of cotranslational translocation of vascular cell adhesion molecule. *Nature* **2005**, *436*, 290–293.

(45) Williams, D. H.; Stephens, E.; OBrien, D. P.; Zhou, M. Understanding noncovalent interactions: ligand binding energy and catalytic efficiency from ligand-induced reductions in motion within receptors and enzymes. *Angew. Chem., Int. Ed.* **2004**, *43*, 6596–6616.

(46) Whitesides, G. M.; Krishnamurthy, V. M. Designing ligands to bind proteins. *Q. Rev. Biophys.* **2005**, *38* (4), 385–395.

(47) Williams, D. H.; Stephens, E.; Zhou, M. Ligand binding energy and catalytic efficiency from improved packing within receptors and enzymes. *J. Mol. Biol.* **2003**, *329*, 389–399.

(48) Baum, B.; Muley, L.; Smolinski, M.; Heine, A.; Hangauer, D.; Klebe, G. Non-additivity of functional group contributions in protein−ligand binding: a comprehensive study by crystallography and isothermal titration calorimetry. *J. Mol. Biol.* **2010**, *397*, 1042–1054.

(49) Hilgeroth, A.; Molnur, J.; De Clercq, E. Using molecular symmetry to form new drugs: hydroxymethyl-substituted 3,9-diazatetraasteranes as the first class of symmetric MDR modulators. *Angew. Chem., Int. Ed.* **2002**, *41*, 2623–3625.

(50) Sanmartín, C.; Font, M.; Palop, J. A. Molecular symmetry: a structural property frequently present in new cytotoxic and proapoptotic drugs. *Mini-Rev. Med. Chem.* **2006**, *6*, 639–650.

(51) Lemm, J. A.; OBoyle, D., II; Liu, M.; Nower, P. T.; Colonno, R.; Deshpande, M. S.; Snyder, L. B.; Martin, S. W.; St. Laurent, D. R.; Serrano-Wu, M. H.; Romine, J. L.; Meanwell, N. A; Gao, M. Identification of hepatitis C virus NS5A inhibitors. *J. Virol.* **2010**, *84*, 482–491.

(52) Gao, M.; Nettles, R. E.; Belema, M.; Snyder, L. B.; Nguyen, V. N.; Fridell, R. A.; Serrano-Wu, M. H.; Langley, D. R.; Sun, J.-H.; OBoyle, D. R., II; Lemm, J. A.; Wang, C.; Knipe, J. O.; Chien, C.; Colonno, R. J.; Grasela, D. M.; Meanwell, N. A.; Hamann, L. G. Chemical genetics strategy identifies an HCV NS5A inhibitor with a potent clinical effect. *Nature* **2010**, *465*, 96–102.

(53) Bell, T. W. Drugs for hepatitis C: unlocking a new mechanism of action. *ChemMedChem* **2010**, *210*, 1663–1665.